Time-Dependent Sensitivity Analysis of Biological Networks: Coupled MAPK and PI3K Signal Transduction Pathways†

Dawei Hu‡ and Jian-Min Yuan*,‡

Department of Physics, Drexel University, Philadelphia, Pennsylvania 19104-2875

Received: October 27, 2005; In Final Form: December 23, 2005

Sensitivity analysis has been widely used in the studies of complicated chemical reaction and biological networks, for example, in combustion studies and metabolic control analysis of pathways. In the latter cases, the responses of system properties at steady states with respect to changes of parameters, such as initial concentrations and rate constants, are often expressed as sensitivities. Besides steady-state sensitivities, time-dependent sensitivities should be useful; however, the explicit use of them in analyzing complicated biological systems has so far been limited. Using the coupled mitogen activated protein kinase (MAPK)−phophatidylinoisitol 3′-kinase (PI3K) system of the Ras pathways, known to be involved in about 30% of human cancers, as an example, we show that time-dependent sensitivities are useful for the studies of complex biological systems. They provide, for example, the following information: (a) multiple time scales existing in a complex system involving cross-talks and feedback loops; (b) the signs and strengths of responses to perturbations (as system complication increases, the signs of global responses are not always easily determined; for example, response may change sign more than once as time evolves); (c) beyond concentration dynamics, sensitivities revealing further details about the intricate dynamics and the effects of the cross-talks; (d) ranking of vulnerability of nodes of a biological network using integrated sensitivity—a first step toward the identification of drug targets; (e) reduced sensitivity serving as a measure of the stability or robustness of pathways. Our results indicate that the role of the PI3K branch in the coupled pathways is to enhance the robustness of the MAPK pathway. More importantly, they demonstrate that time-dependent sensitivity analysis can be a valuable tool in system biology.

I. Introduction

The application of sensitivity analysis in the studies of complicated chemical and biological networks has a long history.[1−4] In chemical kinetics, the associated techniques have been applied to combustion,[5] atmospheric chemistry,[6] the determination of parameters of potential energy surfaces,[7] biomolecular simulations,[8,9] etc. The tool of sensitivity analysis speeds up the processes in identifying the key parameters that control the behavior and performance of the entire systems. This is achieved by calculating simultaneously many derivatives, instead of changing parameters one step and one variable at a time. For biological networks, sensitivities have been extensively used in the studies of metabolic pathways.[3,4] In particular, various types of sensitivity derivatives are defined in the metabolic control analysis (MCA) and summation and connectivity theorems associated with them established.[3,4] However, applications of similar types of analyses to cellular signaling pathways are relatively rare, as discussed in several recent papers.[10−12] In most MCA as well as applications to signaling pathways, steady-state sensitivities are often used. The potential usage of time-dependent sensitivities along non-steady-state trajectories[12] has rarely been explored.

Because abnormalities of signaling pathways are involved in many diseases, such as cancers, diabetes, depression, etc., and our knowledge of the enzymatic reactions involved in these pathways are improved daily, some pathways have become so well-defined that it is worthwhile to simulate them in silico. In fact, it may be necessary for the close collaboration between experimental, theoretical, and simulation studies to determine eventually the correct reaction kinetic steps as well as the protein−protein interactions, cross-talks, and feedback loops existing in pathways. The importance of signaling pathways demands us to use all the tools that are available to reveal their functionality and dynamic behaviors as detailed as possible. It is the purpose of this article, using the coupled MAPK-PI3K pathways as an example, to show that the time-varying sensitivity analysis is a valuable tool in this regard.

In the following paragraphs, we briefly describe the nature of the complicated Ras signaling network in general and the coupled MAPK-PI3K pathways in particular. The Ras signaling network[13,14] plays an important regulatory role in controlling cell proliferation, differentiation, cell survival, and apoptosis. Cancer occurs when normal cell growth regulation breaks down.[15,16] Such breakdown is often attributed to an accumulation of defects in one or more signaling pathways. Ras oncogenes and their coded proteins are among the first molecules identified as effectors of pathways regulating cell growth and death.[14] Studies show that about 30% of all human tumor growth is related to mutations of the Ras protein.[15,16] This number is likely to be even higher, if one considers all effectors in the Ras-related signaling pathways.

Among the Ras pathways, the most well studied is the mitogen activated protein (MAP) kinase cascade,[17−21] which includes a sequence of enzymes serving as kinases (activators) and their associated phosphatases (deactivators). The first

† Part of the special issue "John C. Light Festschrift".

‡ E-mail address: Dawei.Hu@drexel.edu (D.H.); yuanjm@drexel.edu (J.M.Y.).

10.1021/jp0561975 CCC: $33.50
Published on Web 02/16/2006

downstream kinase from Ras is Raf, which is activated at the intracellular membrane by the GTP-bound Ras.[22−24] In turn, Raf activates MEK, which activates ERK, forming a cascade of MAPK that amplifies the external signal.[17−21] Activated ERK then translocates to the nucleus and activates transcription factors,[25] which regulate the transcription processes. Because the MAPK cascade controls cell growth, survival and apoptosis and dysregulation of their kinases and phosphatases may result in cancer formation, many of its effectors (kinases and phosphatases) have been considered as targets for therapeutic intervention for cancers.[26]

The network of human cellular pathways is very complex and many parallel pathways are interacting with one another.[13,14] Most pathways have not yet been mapped out and the cross-talks that act between them are so far largely unknown. For the purpose of developing an understanding of how protein interaction networks work, subsets of these pathways are often considered. Several pathways are known to interact with the MAPK pathway to regulate, enhance or inhibit its functions.[26] The most important one among them could be the PI3K and Akt pathway (PI3K/Akt). However, the cross-talks between them are complicated.[27] In fact, PI3K seems to play contradictory roles in regulating MAPK signals; sometimes it is to enhance the signal, other times to inhibit its signal,[27] depending on the details of the connections and phosphorylation. In the present article, we shall analyze the model proposed by Hatakeyama et al. for heregulin (HRG)-induced ErbB receptor signaling,[19,20,28] where a direct cross-talk between the MAPK and PI3K pathways exists through Akt deactivation of Raf via Ser259 phosphorylation and an indirect cross-talk exists that is created by the double functions of a phosphatase, protein phosphatase 2A (PP2A), which deactivates both MEK (MAPK/ERK kinase) and Akt, where ERK stands for extracellular signal-regulated kinase. The Hatakeyama model is developed on the basis of experiments done on Chinese-hamster ovary cells expressing ErbB4 receptors.[28]

The organization of the article is as follows: The model of Hatakeyama et al. for coupled MAPK and PI3K pathways[28] is described in section II along with a modular representation of the model that we have introduced. Concentration dynamics of some pathway proteins, which exhibit amplification and delay, are presented in section III, setting up the reference frame for later discussion of sensitivities. Time-dependent sensitivities of effector concentrations to rate parameters and initial conditions are defined and numerically solved using symbolic differentiation methods in section IV. These sensitivities are used to reveal the details of the effects of cross-talks on effector dynamics. In section V, we rank the vulnerable points (or drug targets) of the pathways using integrated sensitivities. Because robustness and redundancy are often properties associated with design principles of natural biological network, we examine the robustness of MAPK/PI3K pathways using integrated sensitivities in section VI, which is followed by a conclusion and discussion section.

II. Coupled MAPK and PI3K Pathways

The model we study in the present article is that proposed by Hatakeyama et al.,[28] which comprises primarily two pathway branches activated by the ligand-induced and tyrosine-phosphorylated ErbB4 receptor (R). One is the Ras-Raf-MEK-ERK cascade pathway (also known as the MAPK pathway) and the other is the PI3K-Akt pathway, which regulates the MAPK pathway. Both pathways are initiated when heregulin (HRG) binds to the receptors, which are then dimerized and transphosphorylated to form phosphorylated receptor (RP).

The phosphorylated ErbB4, RP, is known to bind competitively with Src-homology and collagen domain protein (Shc) and with the p85 subunit of the phophatidylinoisitol 3′-kinase (PI3K).[29−31] Binding of RP to Shc (to form R-Shc) initiates the MAPK pathway. This is achieved by complex formation and dissociation with adapter proteins (e.g., Shc, GS). Details can be found in Hatakeyama et al.[28] and are summarized in a schematic modular diagram in Figure 1. Focusing on the MAPK cascade, we just mention that the adapter ShGS complex accelerates the GDP-GTP exchange on Ras. The activated form, RasGTP, then activates Raf, which is deactivated by an unknown enzyme "E"[28,32] as well as by Akt-PI-PP, an effector of the PI3K-Akt pathway. As in a standard MAPK cascade, activated Raf (Raf*) then activates the downstream kinase MEK, which then activates ERK. In both of these cases, phosphorylation and dephosphorylation are done through a double phosphorylation−dephosphorylation cycle (DPdPC). This is all shown in the schematic diagram of the pathways, which for the convenience of analysis are divided into eight modules. More details are given later in the section.

The other branch, the PI3K-Akt pathway, is activated when HRG-stimulated receptor (RP) binds to the SH2 domain on the p85 subunit of PI3K. This is achieved through the activation of Akt, which is recruited to the inner surface of the plasma membrane by phosphatidylinositol-3,4,5-triphosphate (PIP3). Akt is fully activated through a double phosphorylation process catalyzed by 3′-phosphoinositide-dependent protein kinase 1 (PDK) and deactivated by PP2A. This pathway can also be switched off through deactivation of PIP3 by phosphatase and tension homologues (PTEN).

In the present model, the coupling between the MAPK and PI3K-Akt pathways is through Raf's deactivation at Ser259[28,33,34] by PIP3-bound doubly phosphorylated form of Akt (Akt-PI-PP). There exists actually another more subtle cross-talk between the two pathways, which arises from the fact that phosphatase PP2A catalyzes the deactivation of both MEK and Akt. The dual function of PP2A causes a competition for PP2A by the MEK and Akt double phosphorylation and dephosphorylation cycles. As a result, activation of one inhibits the activation of the other. We will refer to this latter type of cross-talk as PP2A sharing. The competitive and balancing effects of these two types of cross-talks on the dynamics and sensitivity of the MAPK/PI3K pathways are one important aspect of the present study.

As shown in Figure 1, we have divided the coupled MAPK and PI3K pathways into eight modules,[35] which from top down and left to right are: the RP module, the Shc module, the PI3K module, the Ras, Raf, MEK, ERK modules, and the Akt module. Our definitions of these four Ras-Raf-MEK-ERK modules follow those of Kholodenko et al.,[10] who defined simple modules as those that have one communicating effector as input and one communicating effector as output. However, this module definition needs to be expanded to include multiple inputs and outputs[10] for complicated networks as the present one. For instance, the Raf module sitting at the crossroad of pathways has three inputs and one output and, therefore, is not a simple module. As shown, each of the Ras and Raf modules contains a phosphorylation−dephosphrylation cycle (PdPC) and each of the MEK and ERK modules consists of a DPdPC. The Akt module contains a PdPC of PI, binding of Akt and PIP3, and a DPdPC of Akt-PIP3. Finally, in Figure 1, the numbers attached to connection edges denote the reaction numbers, which are defined by Hatakeyama et al.[28] and are often referred to in the present article.

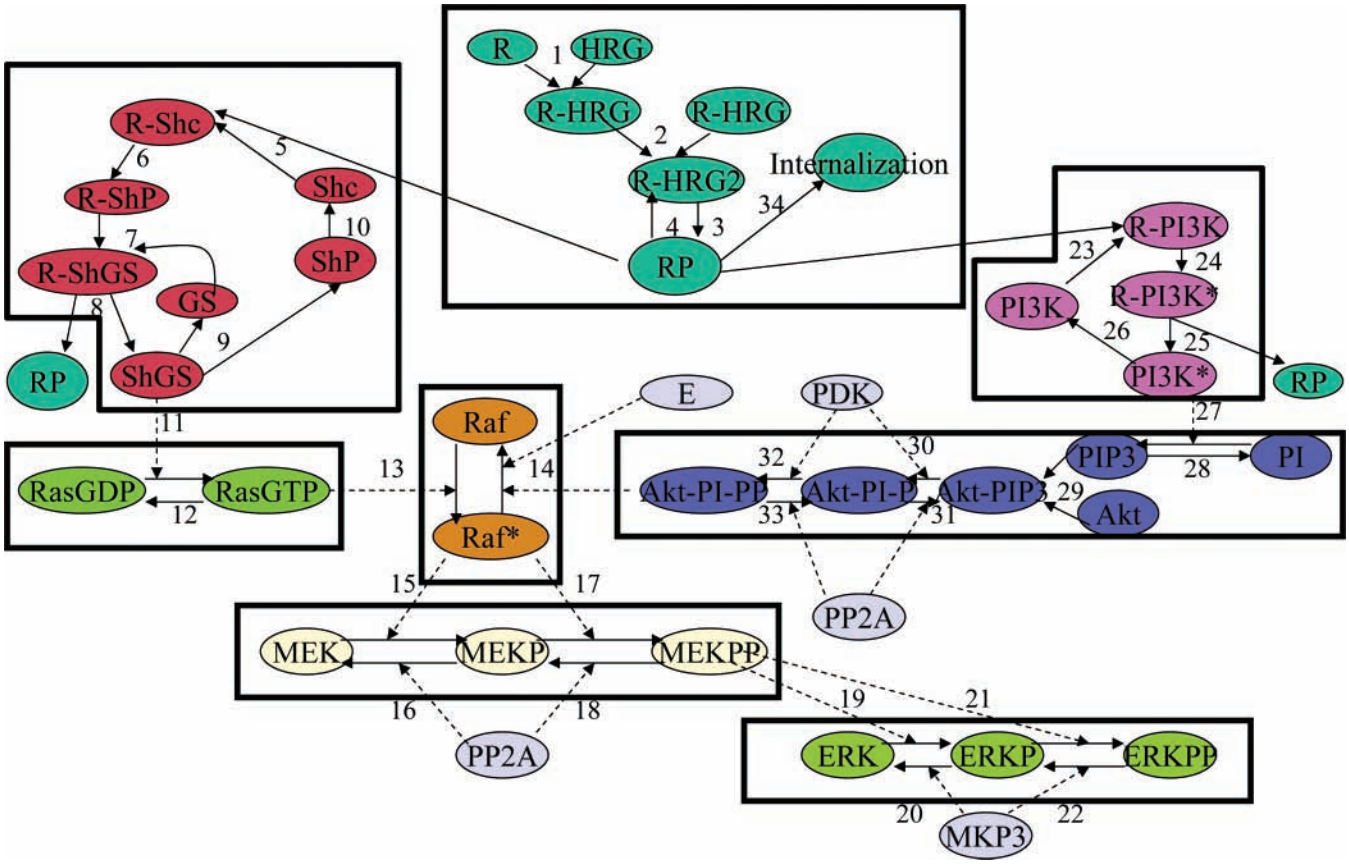

Figure 1. Coupled MAPK and PI3K pathways separated into modules. The numbers on the connection arrows denote the reaction numbers referred to in the text (see ref 28). A number located between two converging arrows denotes two protein molecules reacting to form a protein complex. This includes reactions 1, 2, 5, 7, 23, and 29. A number located between two diverging arrows denotes a protein complex dissociating into two protein components. This includes reaction 8, 9, and 25. Furthermore, as examples, k_5 corresponds to the rate constant of the complex formation of R-ShP from RP and Shc and k_{-5} is the rate constant for the complex dissociation. The symbol k_9, on the other hand, denotes the rate constant of complex dissociation of ShGS into ShP and GS, and k_{-9} is the rate constant for the complex formation. Designations:

HRG: Heregulin
R: ErbB4 receptor
R-HRG: HRG-bound ErbB4 receptor
R-HRG2: $(\text{R-HRG})_2$, dimerized receptor
RP: tyrosine-phosphorylated receptor
Shc: Src-homolog and collagen domain protein
ShP: Shc-P (phosphorylated Shc)
R-Shc: RP-Shc
R-ShP: RP-Shc-P (phosphorylated RP-Shc complex)
GS: Grb2-SOS
ShGS: Shc-Grb2-SOS
R-ShGS: RP- Shc-Grb2-SOS
RasGDP: GDP-bound Ras
RasGTP: GTP-bound Ras
Raf: Raf-1 Mitogen-activated protein kinase kinase kinase
Raf*: Ser^{259} dephosphorylated Raf-1
MEK: MAPK/ERK kinase or Mitogen-activated protein kinase kinase
MEKP: singly phosphorylated MEK
MEKPP: doubly phosphorylated MEK
PP2A: protein phosphatase 2A
ERK: extracellular signal-regulated kinase
ERKP: singly phosphorylated ERK
ERKPP: doubly phosphorylated ERK
MKP3: MAPK phospatase 3
PI3K: phosphatidylinositol 3-kinase
R-PI3K: RP-PI3K
R-PI3K*: RP-PI3K-P
PI3K*: PI3K-P
PI: phosphatidylinositol
PIP3: phosphatidylinositol-3,4,5-trisphosphate
Akt: serine/threonine kinase
Akt-PIP3: PIP3-bound Akt
Akt-PI-P: singly phosphorylated PIP3-bound Akt
Akt-PI-PP: doubly phosphorylated PIP3-bound Akt
PDK: PDK1, 3-phosphoinositide-dependent protein kinase
E: unknown enzyme
RP_internalization: internalized RP

III. Concentration Dynamics of Effectors

To set up a reference frame for the discussion of the time-dependent sensitivities, we first characterize the dynamic behaviors of effector concentrations in this coupled pathway system. Dynamic behaviors are obtained by solving the chemical kinetic equations[28] numerically. Let **x** be a column vector of the concentrations of the effectors, **p** represents a parameter vector, and **k** be the vector of the rate constants and Michaelis−Menton rate parameters.[3] The chemical kinetic equations of the coupled pathway system can then be written as

$$\frac{d\mathbf{x}}{dt} = \mathbf{F}(\mathbf{x},\mathbf{p}) \qquad (1)$$

where **F** is a vector of functions, $\{F_i\}$, defining the rates, $\mathbf{x} = (x_1, x_2, ..., x_N)$, and $\mathbf{p} = (\boldsymbol{p}_1, p_2, ..., p_M) = (\mathbf{k}, \mathbf{x}(0))$. The number of effectors, N, explicitly represented in the equations is 36, whereas the total number of parameters, M, is 82, of which 68 are rate constants or Michaelis−Menton rate parameters and 14 are nonzero initial effector concentrations, as given by Hatakeyama et al.[28] The rest of the initial concentrations are all set to zero. If not otherwise specified, all of our dynamic results presented below are based on this set of initial conditions of effector concentrations. To obtain dynamic behavior of effectors of the pathways, we solve eq 1 on computers (SUN V880) using numerical algorithms. Several algorithms (see section IV) are used for comparison and checking of accuracy.

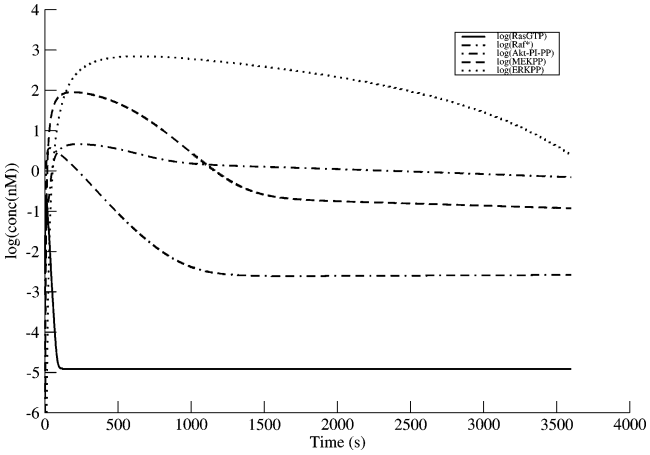

Figure 2. Amplification and delay of downstream signals shown in the time series of RasGTP, Raf*, MEKPP, ERKPP, and Akt-PI-PP concentrations. Logarithmic values are plotted and the curves are denoted by RasGTP (solid line), Raf* (2 dashed lines with 1 dotted line), Akt-PI-PP (1 dashed line with 1 dotted line), MEKPP (dashed line), and ERKPP (dotted line). The reactions and rate constants are the same as Hatakeyama et al.[28]

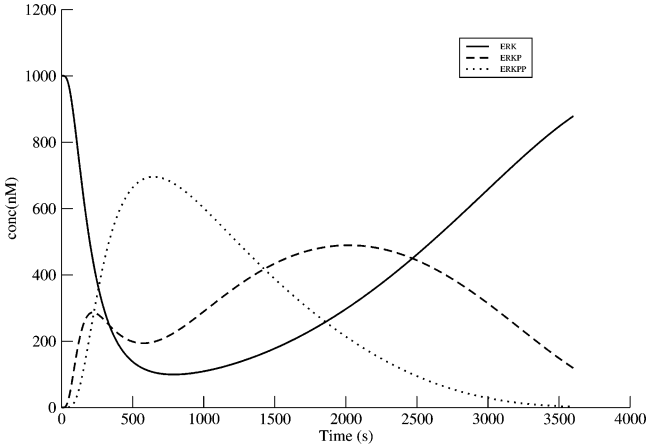

Figure 3. Competition dynamics of the ERK cycle. The reactions and kinetic parameters are the same as Figure 2. The ERK cycle includes time ERK (solid line), ERKP (dashed line), and ERKPP (dotted line).

To characterize the dynamic behaviors of effector concentrations, we first investigate the behavior of signal amplification and delay of the MAPK cascade, as exhibited by the present MAPK-PI3K coupled system. Figure 2 shows the delayed responses of downstream effectors as compared to their upstream effectors. The peaking times of the effectors concentration dynamics appear in the following order: RasGTP < Raf* < MEKPP < Akt-PI-PP < ERKPP. This is the expected behavior of the MAPK cascade (that is, upstream kinases peak ahead of downstream ones) with the additional information on Akt.

The signaling strength of a kinase is determined not only by its maximal intensity but also by the duration of the signaling. Thus, the integrated area under the concentration curve is a better measure of the overall signal strength, according to which an amplification factor can be defined as the ratio of the downtream effector area over the upstream one. Based on this criterion, the amplification factor from RasGTP to Raf* is 206, that from Raf* to MEKPP is 68.2, and that from MEKPP to ERKPP is 23.2, so the overall strength of ERKPP is amplified about 3×10^5-fold over that of RasGTP.

We have also examined the competition dynamics within the MEK and ERK cycles. In these DPdP cycles, the substrates are phosphorylated by their kinases (Raf* in the MEK cycle and MERPP in the ERK cycle) and dephosphorylated by their phosphatases (PP2A in the MEK cycle and MKP3 in the ERK cycle). In Figure 3, the concentrations of ERK, ERKP, ERKPP are plotted as a function of time and the MEK cycles show similar behavior; for example, in both the singly phosphorylated substrate shows double peaks.

The general competition dynamics of these DPdPC cycles can be understood in the following way: Let M stand for the unphosphorylated substrate, MP for the singly phosphorylated, and MPP for the doubly phosphorylated substrate. Initially, when M was phosphorylated, MP starts to rise, and MPP also rises as a result, but at a slower rate. At this time the kinase has a greater effect on the reactions than the phosphatase does. As time goes on, M further decreases and MP has a higher rate to turn into MPP than the rate at which M turns into MP. So MP starts to drop, while MPP still goes up. While this is going on, kinase is going through its own time evolution determined by the upstream cycle right before this one; its concentration decreases to zero at a faster rate. Because of this decay and the simultaneous action of phosphatase, MPP starts to decrease and MP rises again for a second time as a consequence. Because MP is also dephosphorylated by phosphatase, its concentration will drop to approach zero and at the same time the concentration of M rises all the way up to about its initial value and is ready for another round of signaling transduction.

IV. Time-Dependent Sensitivity Analysis

A set of dynamic equations for the time-dependent sensitivities is obtained simply by differentiating both sides of eq 1 with respect to a parameter p_j and can be written as

$$\frac{\mathrm{d}}{\mathrm{d}t}S_{ij} = \sum_l \frac{\partial F_i}{\partial x_l} S_{lj} + \frac{\partial F_i}{\partial p_j} \tag{2}$$

where $S_{ij} \equiv \partial x_i/\partial p_j$ is defined as the sensitivity of the ith chemical species with respect to the jth parameter. Equation 2 is the starting point for sensitivity analysis[1,2,36] and also fundamental equations for metabolic control analysis.[3,4,12,37−39] Similar to the concentration dynamics, we can solve eq 2 for the dynamic developments of sensitivities by numerical algorithms, but here the i-index goes from 1 to 36 and the j-index from 1 to 82; thus we have in all 2952 coupled first-order differential equations to solve. The initial conditions for S_{ij} are $S_{ij} = 0$, unless $p_j = x_i(0)$, in which case $S_{ij} = 1$.[1,12] Presentation and discussion of the calculated results of time-dependent sensitivities in this section are one of the main objectives of the present article. As discussed in the Conclusion and Discussion (section VII), the time-dependent sensitivities in some cases are good approximations to the time-dependent changes in the finite-difference perturbation experiments. Thus their investigations can be, to some extent, related to real experiments.

A. Numerical Methods of Calculating Time-Dependent Sensitivities. Our code is written in such a way that it reads in a description file, which describes the reaction steps, fixes initial concentrations, and specifies the set of sensitivity equations to solve. The code automatically generates the differential equations for the chemical kinetic steps involved as well as the differential equations for the sensitivities. This means that the sensitivity differential equations are generated in the code through symbolic differentiation, not directly read in as an input. This set of differential equations and the set of chemical kinetic equations are then solved simultaneously using numerical algorithms, such as fourth-order Runge−Kutta or semi-implicit extrapolation method.[40] The accuracies of the integrators have

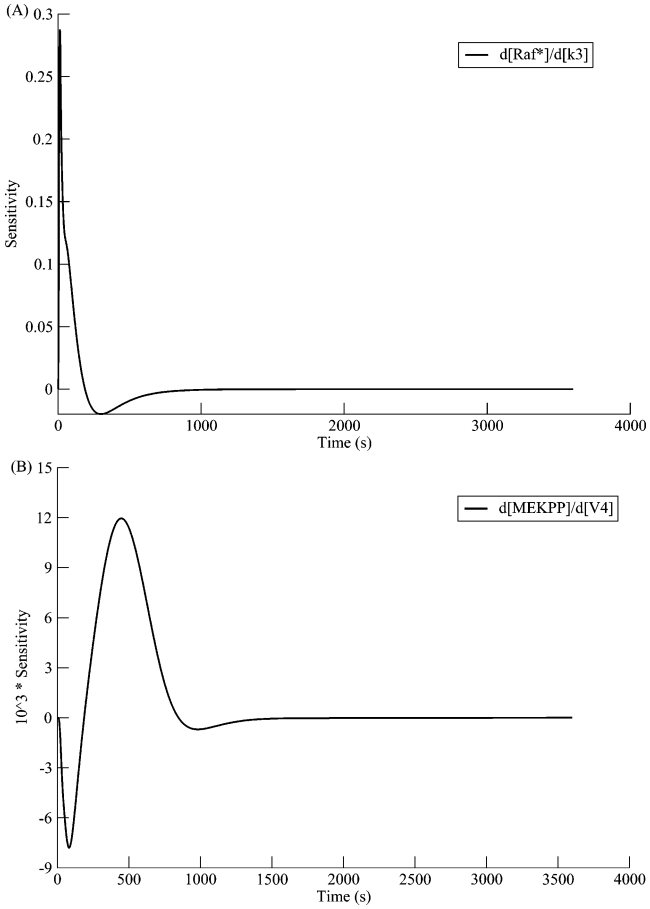

Figure 4. (A) Time-dependent sensitivity of Raf* versus k_3. (B) Time-dependent sensitivity of MEKPP versus V_4.

been checked by comparing results using different numerical methods. Furthermore, the accuracies of the time-dependent sensitivities have also been checked against finite difference calculations in which the value of the parameter (p_j) is varied by a small finite amount.

B. Effects of Cross-Talks on the Sensitivities of Raf* and MEKPP. Raf plays an important role in the MAPK pathway and in the present model its activation is a good indicator of the effects of the direct cross-talk, because it sits at the crossroad of the two branches, as shown in the modular plot, Figure 1. To see how sensitive the activated form of Raf, Raf*, is to an upstream interaction, we have plotted its time-dependent sensitivity with respect to k_3 in Figure 4A. k_3 is the rate constant for the self-phosphorylation of the HRG receptor, R, after HRG attachment and receptor dimerization. Thus the sensitivity of Raf* to k_3 indicates how generation of RP affects generation of Raf*. The phosphorylated receptor, RP, triggers two branches of signal transduction, one of which activates RasGTP and the other activates Akt-PI-PP. RasGTP activates Raf, whereas Akt-PI-PP as well as enzyme 'E' deactivate Raf*, by converting Raf* back to Raf. Figure 4A reveals two properties of the pathways: the sensitivity of Raf* to k_3 goes through a sign change as time evolves and the positive response comes before the negative one. The interpretation of the results is: As shown in Figure 2 that RasGTP reaches its peak value far earlier than Akt-PI-PP does. So when the number of RP increases, more RasGTP is generated first than Akt-PI-PP is. At this stage, more RP means more RasGTP, and thus more Raf*. Therefore, the early response of Raf* with respect to k_3 is positive. When RasGTP is converted to RasGDP and its concentration decreases to close to zero, at the same time the concentration of Akt-PI-PP approaches its peak value. Thus the sensitivity curve decreases as a function of time and becomes negative, for Akt-PI-PP deactivates Raf*. The fact that the time-dependent sensitivity curve in Figure 4A first shows a (sharp) positive peak and then decreases to become a (shallow) negative valley tells us that the time scale of the signal transduction via the Shc-RasGTP branch is much faster than that of the PI3K-Akt branch. This is a desired property, probably an underlying design principle of the Ras pathways, because one of the roles of the PI3K-Akt branch is to switch off or regulate the activation of the MAPK cascade stimulated by the external (HRG) signal.

A few remarks about the sensitivities of other effectors with respect to k_3 can be made. As a function of time, the sensitivity curve of RasGTP with respect to k_3 also changes sign from positive to negative. The reason that the sensitivity of RasGTP changes sign from positive to negative is different from that of Raf*. The sign change of Raf*'s sensitivity is not because of the effect of RasGTP's sensitivity over k3. Because without the PI3K branch, RasGTP's sensitivity goes up and down, but Raf*'s is always positive. It is, instead, attributed to the shift of the equilibrium of the complex dissociation reaction, R-ShGS $\rightleftarrows$ RP + ShGS, when the concentration of RP becomes higher. In contrast to the sensitivity curve of Raf*, those of MEKPP and ERKPP stay positive for the whole time, where a small positive peak followed a larger positive peak. The fact that the second peak is positive is surprising in view of the behavior of Raf*, but it can be explained by PP2A sharing, discussed in the next subsection IV.C. The main reason is that increasing Akt-PI-P and Akt-PI-PP concentrations use up more PP2A, thus less PP2A is available for the deactivation of MEKPP.

As another example, we examine the responses of MEKPP to the change of V_4, the Michaelis−Menton limiting rate at which the phosphorylated ErbB4 receptor, RP, is deactivated to a dimer of the HRG-receptor complex. Figure 4B shows that the response of MEKPP is characterized by one peak and two valleys. To understand their origins, we note that the effect of V_4 is similar that of k_{-3}, the backward rate constant for the phosphorylation of the dimer receptor. Thus we expect qualitatively MEKPP's response is the negative of the Raf* response shown in Figure 4A. This explains the first valley followed by a peak. However, an additional second valley following the positive response appears in Figure 4B and is attributed to the effect of PP2A sharing (more details discussed in subsection IV.C). Because, as can be seen in Figure 2, by the time the second negative valley arrives, RasGTP is long gone; however, the concentrations of MEKPP and Akt-PI-PP are still appreciable. Less RP means less Akt-PI-PP, thus more PP2A available to deactivate MERPP; thus the effect is negative. The disappearing times of MERPP in Figure 2 and of its sensitivity toward PP2A as shown later Figure 6 are roughly consistent with the timing of the second negative valley in Figure 4B. (Sensitivity data and plots of all the effectors with respect to k_3, V_4, k_{27}, k_{11}, only some of which are reported in this article, are available to interested readers, who can contact us using the e-mail addressess listed in the article.)

In short, these two examples show that, in general, time-dependent sensitivities can be used to provide information on time scales of dynamical processes as well as signs of responses to parameter changes. An additional comment is that when we examine a sequence of upstream and downstream effectors (ShGS, RasGTP, Raf*, MEKPP, ERKPP) to the same rate parameters, such as V_4, we see that, as in concentration dynamics (as shown in Figure 2), the sensitivity responses also exhibit signal amplifications and peak delays. Thus a small sensitivity

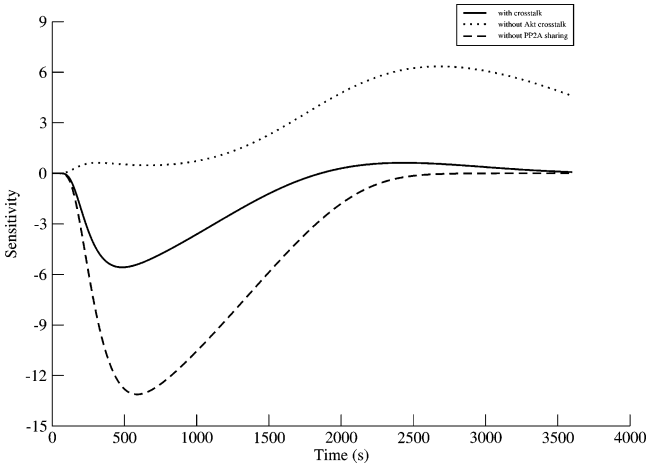

Figure 5. Effects of Akt-Raf cross-talk and PP2A sharing on the sensitivity dynamics of ∂[ERKPP]/∂k_{27}. The time series plotted are cases for a system with the Akt-Raf cross-talk and PP2A sharing (solid line), without Akt-Raf cross-talk, but with PP2A sharing (dotted line), and with Akt-Raf cross-talk, but without PP2A sharing (long dashed line). The rate constants and kinetic parameters used are the same as those of Hatakeyama et al.,[28] except that the initial concentration of Akt is set to 40 nM.

of an upstream effectors can induce large amplified sensitivities in the downstream effectors.

C. Effects of the Akt-Raf Cross-Talk and PP2A Sharing on Dynamics. ERKPP is the key signal of the MAPK pathway, which is translocated to the nucleus to activate transcriptional factors. It is thus important to study its sensitivities to various parameters. In this subsection, the sensitivity of ERKPP to the cross-talk of the coupled system is examined and, specifically, the sensitivity of ERKPP to k_{27} is used as an indicator. The results are plotted in Figure 5.

We first note that k_{27} is the k_{cat} (turnover number)[3] of the enzymatic reaction in which PI3K catalyzes the PI → PIP3 reaction. PIP3 is in turn an intermediate that eventually leads to the production of Akt-PI-PP. On the basis of this fact, one would have conjectured that the sensitivity was always negative. But this turns out not to be the case. As mentioned earlier, there exists another element of the cross-talk in the scheme, which arises from the fact that PP2A serves as the common phosphatase for both the MEK and Akt cycles. As a result, MEKP, MERPP, Akt-PI-P, and Akt-PI-PP compete for PP2A through the enzyme−substrate complex formation processes. Higher concentrations of Akt-PI-P and Akt-PI-PP would mean less PP2A available to deactivate MEKPP (and MERPP), and thus higher ERKPP produced; this is positive sensitivity. To see the separate actions of these two elements of cross-talk, we have plotted in Figure 5 the time-dependent sensitivities for three cases: with both elements present, switching off the Akt-PI-PP and Raf* interaction, and switching off the PP2A cross-talk. The results show that the effect of the Akt-PI-PP and Raf* cross-talk alone is always negative, that due to PP2A sharing is mainly positive, and the combined effect is that the sensitivity is first negative and then becomes positive. The fact that it is first negative, then positive, also tells us about the timings of the competing processes; the positive effect on ERKPP due to PP2A sharing lags behind the negative effect due to Akt-Raf* cross-talk by more than 1000 s. As to the double-peaked nature of the ERKPP sensitivity (with only PP2A sharing) curve, we have traced its origin and attribute it to the fact that its precursor, ERKP, is double-peaked as seen in Figure 3.

D. Sensitivities of MEK, MEKP, MEKPP with Respect to PP2A. To see the effects of phosphatase in a double phosphorylation−dephosphorylation cycle, we have plotted in Figure 6 the sensitivities of MEK, MEKP, and MEKPP to the initial concentration of PP2A. Because PP2A catalyzes the MEKPP → MEKP and MEKP → MEK reactions, higher PP2A concentration implies more MEK is produced and more MERPP is deactivated. So MEK has positive sensitivity with respect to PP2A's initial concentration, and MEKPP has negative sensitivity. This prediction agrees with the results shown in Figure 6. Furthermore, because PP2A deactivates MEKP into MEK, and MEKPP into MEKP, the sensitivity of MEKP against PP2A's initial concentration should be the negative of a combination of the MEK and MEKPP sensitivities. This fact is dictated by the mathematical equations (eq 2) and verified in Figure 6. Initially, MEKPP's sensitivity dominates and is negative, so MEKP's sensitivity is positive. When MEKPP's sensitivity gradually goes down to zero, MEK's sensitivity goes up from zero and becomes dominating. So MEKP's sensitivity turns from positive to negative.

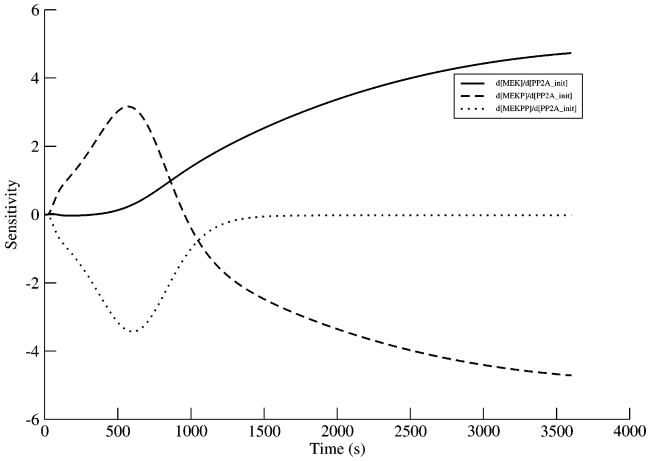

Figure 6. Time-dependent sensitivities of MEK (solid line), MEKP (dashed line), and MEKPP (dotted line) with respect to PP2A's initial concentration.

E. Sensitivities of the ERK Cycle to Upstream Kinase Rate Parameters. In section III, we show the competition dynamics between the concentrations of the DPdPC effectors, in this subsection we investigate how their sensitivities with respect to the rate parameters of upstream kinases vary with time. As an example, the sensitivities of ERK, ERKP, and ERPP with respect to k_{11}, k_{cat} for the activation of Ras by ShGS, are plotted in Figure 7. We see there that the sensitivity dynamics are even more fluctuated than those of the concentrations (Figure 3). To analyze the details of these curves, we note that the ERK sensitivity curve stays negative throughout the entire period, but instead of one minimum, as in its population dynamics (Figure 3), it has two minima, revealing the two time scales existing in the dynamics. Along with this two-minimum feature, two maxima are also observed in the ERKPP sensitivity curve, where a second maximum appears as a shoulder of the first maximum. The curve, however, stays positive for the entire period. The ERKP curve does change sign; it begins with a sharp positive maximum, followed by a broad negative well, and then a broad second positive maximum. The signs of ERK, ERKP, and ERKPP are all consistent with the underlying dynamics. Increasing k_{11} corresponds to increasing RasGTP, thus increasing the Raf* activity and increasing the MERKPP signal. Therefore the increasing amount of ERK is converted to ERKP, which is then converted to ERKPP. So, the ERK sensitivity stays negative and the ERKPP sensitivity stays positive, but the ERKP sensitivity changes sign from positive to negative

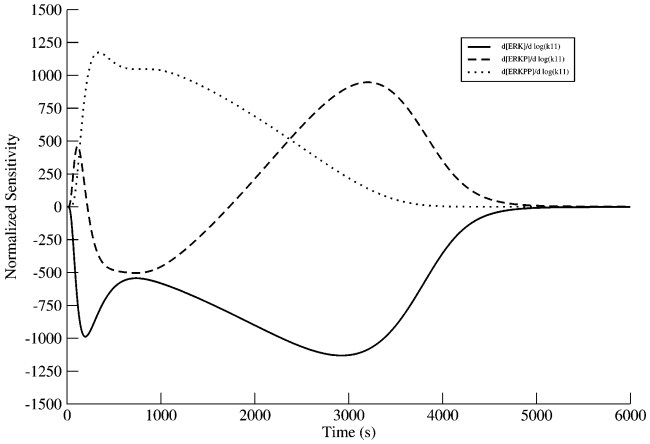

Figure 7. Time-dependent sensitivities of the ERK cycle with respect to an upstream kinase rate parameters k_{11}: ERK (solid line), ERKP (dashed line), and ERKPP (dotted line).

and then back to positive. We note that, as in the MEK cycle (Figure 6), the sensitivity of ERKP is the negative of the sum of the sensitivities of ERK and ERKPP, as dictated mathematically by eq 2. The physical reason for the fluctuations of the ERKP sensitivity is that ERKP first increases when ERK is converted into it; then, when enough ERKP is accumulated, it starts to be converted to ERKPP. Therefore, sensitivity becomes negative. When the ERKPP concentration becomes high enough, it is dephosphorylated to yield ERKP. Thus the ERKP sensitivity becomes positive again. The observation that the maximum of the ERK sensitivity curve corresponds to the negative minimum of the ERKP sensitivity arises from the fact that when an appreciable amount of ERKP is converted to ERK, the ERK sensitivity becomes less negative.

Results in this subsection show that sensitivity curves show more fluctuations thus reveal more details about the time scales and interacting strengths of underlying competing mechanisms than the population dynamics themselves.

V. Lists of Vulnerable Points of the Pathways According to Integrated Sensitivities

Besides their use to improve our understanding of the dynamics and interactions of pathways, time-dependent sensitivities can also be used to rank the most sensitive reaction steps or initial concentrations of the pathways. In other words, we rank the vulnerable points of the pathways using sensitivities. Similar rankings have been done using finite differences.[41] If these vulnerable points are realized experimentally, for example, if oncogenic mutations or over- or underexpression of some effectors are found to be associated with certain diseases, then these reaction steps or initial concentrations can be considered to be potential drug targets. Because ERKPP is an effector translocated into the nucleus to regulate transcription and the abnormality of the ERKPP regulation is considered to be a potential cause of tumor growth, we shall use the ERKPP signal to rank the vulnerable points. We shall consider the sensitivities of ERKPP with respect to the rate constants, Michaelis−Menton parameters of the reactions, or nonzero initial concentrations. In the ranking of sensitivities, a quantity, such as ∂ [ERKPP]/∂ log(p_j), which has the dimension of ERKPP concentration, can be used for common measure. This is preferred, because all parameters are not of the same dimensionality. (The commonly used, dimensionless quantity, ∂ log[ERKPP]/∂ log(p_j), has the difficulty of numerical instability, caused by division by a concentration approaching zero.) The ranking is done using the integrated sensitivity, that is, the area under the time-dependent sensitivity curve integrated over time, because it represents a measure of the accumulated effects of a parameter on ERKPP. The list of the vulnerable points for ERKPP is given in Table 1 in the order of decreasing absolute values of sensitivities, independent of their signs which are also given in the table.

TABLE 1: Vulnerability Ranking of the Coupled Pathways Using Integrated ERKPP Sensitivities

rank (ERKPP)	parameter	value (mM s)	description
1	k_{11}	2.33	k_{cat} for RasGDP → RasGTP
2	V_{12}	−2.29	k_{cat} for RasGTP → RasGDP
3	ERK_{init}	1.80	initial concentration of ERK
4	Shc_{init}	1.68	initial concentration of Shc
5	k_9	−1.59	ShGS → ShP + GS
6	MEK_{init}	1.14	initial concentration of MEK
7	$MKP3_{init}$	−0.90	initial concentration of MKP3
8	k_{14}	−0.88	k_{cat} for Raf* → Raf
9	k_{18}	−0.83	k_{cat} for MEKPP → MEKP
10	k_{22}	−0.79	k_{cat} for ERKPP → ERKP
11	k_{13}	0.77	k_{cat} for Raf → Raf*
12	$K_{m_{14}}$	0.73	K_m for Raf* → Raf
13	$K_{m_{12}}$	0.73	K_m for RasGTP → RasGDP
14	GS_{init}	0.70	Initial concentration of Grb2-Sos
15	k_5	0.69	RP + Shc → R-Shc
16	$PP2A_{init}$	−0.69	Initial concentration of PP2A's
17	k_8	0.68	R-ShGS → RP + ShGS
18	k_{-8}	−0.67	RP + ShGS → R-ShGS
19	$K_{m_{18}}$	0.62	K_m for MEKPP → MEKP
20	E_{init}	−0.60	enzyme *E*'s initial concentration
21	k_{19}	0.57	k_{cat} for ERK → ERKP
22	$K_{m_{19}}$	−0.57	K_m for ERK → ERKP
23	k_{17}	0.48	k_{cat} for MEKP → MEKPP
24	k_{21}	0.45	k_{cat} for ERKP → ERKPP
25	$K_{m_{21}}$	−0.45	K_m for ERKP → ERKPP

A. List of the Vulnerable Points of the Coupled Pathways Using Integrated ERKPP Sensitivities. Table 1 shows some interesting trends. Ranked at top 1 and 2 are the reaction rates related to the activation and deactivation of RasGTP, the first kinase of the MAPK cascade. This can be understood in terms of the amplification property of the cascade. For the same reason, the reaction steps of Raf, MEK and ERK should also rank. Indeed ranked 8−12 are reaction rates related to them and upstream effectors in general rank higher than the downstream effectors. We note also in Table 1 the deactivation steps often rank higher than the corresponding activation steps; thus the model seems to predict that phosphatases may be better drug targets than kinases. This fact may not be useful in reality, because phosphatases often lack specificity. Almost all the reaction parameters ranked in the top 25 in Table 1 are related to the MAKP cascade, except for reactions ranked numbers 5, 15, and 17, which are related to reaction numbers v_5 through v_9, located in the Shc module (see Figure 1). For instance, Reactions v_7, v_8, and v_9 form loops that directly regulate the concentration of the ShGS complex, the kinase for the RasGTP formation. In particular, Reactions v_9 and v_5 rank much higher than what one would expect and thus may be considered as novel vulnerable points predicted by the present model. We note also that reactions v_1 thru v_4 (RP module) and v_{23} thru v_{34} (PI3K and Akt modules) are missing in Table 1.

In Table 1, initial concentrations of some effectors rank high as well. These include kinases, such as ERK and MEK, phosphatases, such as MKP3, PP2A, and E, as well as receptor-complex forming proteins, such as Shc and GS. Again, similarly to v_9 and v_5, initial concentrations of Shc and GS of the ShGS module rank higher than expected.

TABLE 2: Vulnerability Ranking of the Coupled Pathways Using Integrated Akt-PI-PP Sensitivities

rank (Akt-PI-PP)	parameter	value (uM s)	description
1	$PP2A_{init}$	−10.97	PP2A's initial concentration
2	Akt_{init}	7.55	Akt's initial concentration
3	k_{31}	−5.21	k_{cat} for Akt-PI-P → Akt-PIP3
4	V_{30}	5.21	V_m for Akt-PIP3 → Akt-PI-P
5	$K_{m_{30}}$	−5.21	K_m for Akt-PIP3 → Akt-PI-P
6	k_{27}	4.81	k_{cat} for PI → PIP3
7	V_{28}	−4.81	V_m for PIP3 → PI
8	$PI3K_{init}$	4.79	PI3K's initial concentration
9	k_{29}	4.78	Akt + PIP3 → Akt-PIP3
10	k_{-29}	−4.78	Akt-PIP3 → Akt + Pip3
11	$K_{m_{28}}$	4.78	K_m for PIP3 → PI
12	k_{33}	−4.62	k_{cat} for Akt-PI-PP → Akt-PI-P
13	V_{32}	4.61	V_m for Akt-PI-P → Akt-PI-PP
14	$K_{m_{32}}$	−4.61	K_m for Akt-PI-P → Akt-PI-PP
15	$K_{m_{31}}$	3.94	K_m for Akt-PI-P → Akt-PIP3
16	$K_{m_{33}}$	3.63	K_m for Akt-PI-PP → Akt-PI-P
17	k_{11}	2.91	k_{cat} for RasGDP → RasGTP
18	V_{12}	−2.86	V_m for RasGTP → RasGDP
19	R_{init}	2.67	receptor *R*'s initial concentration
20	V_{26}	−2.52	V_m for PI3k* → PI3K
21	$K_{m_{26}}$	2.51	K_m for PI3K* → PI3K
22	k_{23}	2.30	RP + PI3K → R-PI3K
23	Shc_{init}	2.09	initial concentration of Shc
24	k_9	−1.96	ShGS → ShP +GS
25	MEK_{init}	1.72	initial concentration of MEK

Furthermore, a ranking list (not given here) obtained with the entire PI3K pathway branch switched off is very similar to those listed in Table 1. It seems to indicate that the PI3K pathway plays a minor role in the ranking of the ERKPP sensitivities. In other words, the list seems to be robust.

Because the MAPK pathway plays a central role in transmitting proliferating stimuli in a broad range of human cancer cells, the components of the pathway are targets of small-molecule inhibitors. This is an intensely pursued area of research and development in pharmaceutical companies and research institutes.[42,43] Ras was the first oncogene found to be associated with human cancers[14] and was therefore one of the first among all kinases to be identified as a drug target. Here in Table 1 it sits at the top of the list. Following Ras, Raf has become an important drug target recently and inhibitors have also been developed for MEK.[43]

B. List of the Vulnerable Points of the Coupled Pathways Using Integrated Akt-PI-PP Sensitivities. In a similar way, we have ranked the integrated sensitivities of Akt-PI-PP of the full system with respect to all reaction parameters and initial concentrations in Table 2. All the rate and concentration parameters ranked in top 17 (except the initial concentration of PI3K) are related to the effectors in the Akt module (Figure 1). At the top are 2 initial concentrations, those of the phosphatase (PP2A) and a complex-forming protein Akt of the Akt module. These are followed by the rate parameters related to the dephosphorylation and phosphorylation processes of the reaction: Akt-PIP3 → Akt-PI-P, the catalyzed reaction: PI → PIP3 and its dephosphorylated counterpart, and then PI3K. Ranked 17 and 18 are rate parameters related to the RasGTP phosphorylation and dephosphorylation reactions, the highest ranked among all MAPK effectors. The fact that MAPK effectors do not rank higher is not surprising, because they are not upstream effectors of Akt-PI-PP and all effects must come indirectly from the branching from RP and feedback loops involving RP as well as PP2A sharing.

There are experimental evidences relating the effectors listed in Table 2 to cancers and human malignancies. In fact, following MAPK, the PI3K/Akt pathway has emerged as the second hotly pursued pathway.[44] Particularly vulnerable effectors are Akt, PTEN, and PI3K, which are ranked, respectively, (#2−#5, #9, #10, #12−16), (#7 and #11), and (#8, #20−22) in Table 2. Some of experimental facts for them are as follows: Akt's activation and overexpression has been found to correlate with breast, ovarian, thyroid, and pancreatic cancers.[44,45] PTEN, a tumor-suppressing protein, is also identified as an important drug target. Its mutation and silencing is tied to many human malignancies, such as ovarian, breast, melanoma, prostate, lung, hepatocellular renal-cell carcinoma, glioblastoma, thyroid, and lymphoid cancers.[44] Furthermore, two compounds, wortmannian and LY294002, are commonly used as pharmacological agents to indicate PI3K involvement in cancers.

C. Common and Different Features of the Two Ranking Lists. The common features of the ERKPP and Akt-PI-PP sensitivity rankings:

(a) None of the reactions v_1-v_4 involving the receptor (inactivated) and HRG rank at the top 34 in either ranking.

(b) Rate constants k_9 and k_5 as well as initial concentrations of Shc and Gs appear in both lists. On the basis of the present study, these two complex dissociation and formation reactions are vulnerable points, thus potential drug targets.

(c) RasGTP and RasGDP score high in both lists.

(d) Other initial concentrations ranked top 34 in both lists (only the top 25 are shown in Tables 1 and 2) are those of PP2A, MEK and receptor R.

Some differences between these two rankings:

(a) In the ERKPP ranking, the reaction steps involving upstream effectors usually rank higher than the corresponding steps involving the downstream effectors. However, it does not seem to be the case for the Akt-PI-PP ranking. The latter may be correlated with the fact that this is no amplification phenomenon associated with the Akt-PI-PP activation.

(b) Endocytosis of RP ranks at top 26 in the Akt ranking but does not appear in the ERK ranking.

VI. Robustness of Pathways Using Integrated Sensitivities

One of the important goals of scientists studying biological networks and pathways is to learn about their design principles and to compare these principles to those of man-made systems, such as computers, cars, and airplane.[46,47] For instance, robustness and redundancy are often regarded as two of the common properties associated with the design principles of biological networks in nature as well as man-made systems. Biological systems are constantly fluctuating and noisy. To avoid noise-induced transformations, the system should not be sensitive to small fluctuations, that is, be robust in its behaviors. In this section, using the MAPK/PI3K systems again, we want to demonstrate that integrated sensitivities can be used as a countermeasure of the robustness of pathways, because reduced sensitivity may cut down noise-induced transformations. Thus, reduced sensitivity is equivalent to an increase of the threshold of the response to stimulus. The hypothesis here states: the design principle behind the coupled pathways is that the PI3K pathway is to make the MAPK system less sensitive to noise or defects, that is, to counterbalance its ultrasensitivity.[17,48]

To test this hypothesis, we have calculated the integrated sensitivities of the MAPK cascade effectors with respect to certain initial concentrations and rate parameters. Integrated sensitivities are calculated for the full system as well as the system with PI3K pathway switched off. The integrated sensitivities of the cascade effectors, RasGTP, Raf*, MERPP, and ERKPP, are listed in Table 3 in four parts, one each for a

TABLE 3: Integrated Sensitivities of Effectors with Respect to Certain Initial Concentrations and Rate Parameters[a]

effector	I	I_0	$(I_0 - I)/I$ (%)
	(A) Integrated Sensitivities with respect to the Initial Concentration of HRG		
RasGTP	3.2274×10^{-1}	3.2238×10^{-1}	−0.11
Raf*	7.2340×10^{1}	1.1307×10^{2}	56.30
MEKPP	3.3496×10^{3}	4.2352×10^{3}	26.44
ERKPP	8.0980×10^{4}	8.4466×10^{4}	4.30
	(B) Integrated Sensitivities with Respect to the Initial Concentration of R		
RasGTP	7.5645×10^{-1}	7.5241×10^{-1}	−0.53
Raf*	1.3103×10^{2}	2.6394×10^{2}	101.43
MEKPP	7.0501×10^{3}	9.8903×10^{3}	40.29
ERKPP	1.7295×10^{5}	1.9725×10^{5}	14.05
	(C) Integrated Sensitivities with Respect to k_{11}		
RasGTP	9.2792×10^{0}	9.2873×10^{0}	0.09
Raf*	2.0737×10^{3}	3.2456×10^{3}	56.51
MEKPP	9.6198×10^{4}	1.2174×10^{5}	26.55
ERKPP	2.3277×10^{6}	2.4325×10^{6}	4.50
	(D) Integrated Sensitivities with Respect to k_{13}		
RasGTP	0	0	N/A
Raf*	6.8419×10^{2}	1.0691×10^{3}	56.26
MEKPP	3.1868×10^{4}	4.0220×10^{4}	26.21
ERKPP	7.7245×10^{5}	8.0679×10^{5}	4.45

[a] The second column is the effector's integrated sensitivity (I) of the full coupled system, the third column is the integrated sensitivity (I_0) with the PI3K branch switched off, and the fourth column is the difference in integrated sensitivities in percentage.

different parameter. In (A), the sensitivities toward the concentration of the ligand HRG are listed. Listed in (B) are the effector sensitivities with respect to the initial concentrations of the receptor, R. This is motivated by the fact that some cancers are found to be associated with the overexpression of certain receptors in the cell membrane. To simulate the effects of Ras mutations on some downstream effectors, we have listed in (C) and (D) the effector integrated sensitivities toward, k_{11} and k_{13}, the turnover numbers of the Ras and Raf activations, respectively. Table 3 shows clearly that the integrated sensitivities of Raf*, MEKPP, and ERKPP are reduced when the PI3K branch is switched on for all four parameters studied. The percentage differences of sensitivities for these parameters are very close for all parameters, except for R, the initial concentration of receptors. For R, the percentage differences are highest among all, it may indicate that PI3K can protect cells against the risk of overexpression of receptors more effectively. It is also seen that the percentage differences of sensitivities go down rapidly from Raf* to MEKPP to ERKPP.

Table 3 also shows that the integrated sensitivity of RasGTP does not change much with or without the PI3K branch. Their percentage differences are 1−2 orders of magnitude smaller than those of other kinases and can be positive or negative. This is because the MAPK-PI3K cross-talks occur at a point downstream from Ras, thus PI3K branch does not affect it directly. Another measure of reduced sensitivity (not listed) is the change of the signal amplification factor for the whole MAPK cascade. Our results show that this factor is down by 17% for the coupled system compared to the MAPK system alone. Therefore, overall, our results in Table 3 support the notion that the role of the PI3K pathway in the coupled system (as described by the present model) is to reduce the sensitivity or to enhance the robustness of the MAPK pathway.

VII. Conclusion and Discussion

The MAPK-PI3K signaling pathways play an important role in regulating cell functions and mutations of related effectors may be related to cancer formation. To study such complicated signaling pathways, we have developed a general-purpose automation algorithm to compute time-varying sensitivities as well as concentration dynamics. We show that time-varying sensitivity analysis can be a useful tool for systems biology studies of complex biological systems, because it can provide the following valuable information about the systems: (a) competition between multiple time scales existing in a complex system, especially, when cross-talks and feedback loops are involved; (b) the signs and strengths of a system's responses to perturbations mediated by protein−protein interactions and cross-talks; (c) revealing more details of the complex dynamics of the system than concentration dynamics; (d) ranking of vulnerable nodes or potential drug targets of biological pathways using integrations of time-varying sensitivity; (e) reduced sensitivity used as a measure of stability or robustness of pathways (here our results seem to support the notion that the role of the PI3K branch in the coupled MAPK-PI3K pathways is to reduce the integrated sensitivity or to enhance the robustness of the MAKP pathway).

Much of our results and discussions in earlier sections focus on time-dependent sensitivities. One may ask whether any of the observed relations or conclusions are relevant to real experiments. Although time-dependent sensitivities are not directly measured in experiments, the answer, however, is positive. This is because in at least two regimes, the time-dependent sensitivities can be related to experiments investigating effects of finite perturbations.[49,50] The first is the weak perturbation limit; in such a case the differences in time series of the concentrations of the original and perturbed cases are approximately given by the time-dependent sensitivities. The second applicable regime arises when the underlying dynamics behave in the linear domain. In this linear dynamics domain, even when the perturbation is not weak, the finite-perturbation differences are well approximately by the partial derivatives. In practice, we can always use sensitivities as indications of how finite perturbations may work. An advantage of using partial derivatives is that the signs of the derivatives tell us automatically whether the effects are positive or negative.

Although a more complete network involving the MAPK cascade and the PI3K pathway can be much more complicated than the model analyzed in the present article, the Hatakeyama model, however, serves as a useful model for the study of the effects of cross-talks on dynamics. One lesson that we learn from this model is that not only direct protein−protein interactions provide couplings between pathways but also sharing of common phosphatases (or kinases). The situation here is as follows: Although the interaction between Akt and Raf* is to deactivate the latter, the effect of sharing of PP2A between the MEK and Akt cycles on ERK signaling is more subtle. An input that increases Akt activation will negatively regulate Raf, and thus MEK and ERK at an early stage, but this also implies more PP2A is available to deactivate Akt and thus positively regulate Raf as well as MEK and ERK at a later stage. An input that decreases Akt activation has the opposite effects. Furthermore, a perturbation that increases MEK activation also induces a higher rate of MEK-PP2A complex formation; thus less PP2A is available to deactivate Akt. This in turn means lower Raf activation and lower MEK and ERK activation. Therefore, PP2A sharing induces self-regulating or balancing effects on Akt and MEK activation. A point to notice is that redundancy already exists in this model, in the sense both Akt and PP2A can negatively regulate ERK signaling.

Finally, the lists of vulnerability, of course, are as complete as the system that we have simulated in this Article. As already

discussed by Hatakeyama et al.[28] and suggested by works of many others,[16,27,42] the present model can be extended by including more cross-talks and pathways, for example, those connected to Ras, Raf, PI3K, and Akt and even different coexpressed Erb receptors. However, such extensions may require the availability of experimental data of these pathways and protein−protein interactions for the same cell types and same species and obtained under the same protocol.

Acknowledgment. We thank Dr. Mariko Hatakeyama for discussions and sending us their experimental data. This work is partially supported by a Synergy Grant administered by Drexel University, a Sun Microsystems Grant, and a Grant from the Pittsburgh Supercomputer Center.

References and Notes

(1) Rabitz, H.; Kramer, M.; Dacol, D. *Annu. Rev. Phys. Chem.* **1983**, *34*, 419.
(2) Rabitz, H. *Chem. Rev.* **1987**, *87*, 101.
(3) Cornish-Bowden, A. *Fundamentals of enzyme kinetics*; Portland Press: London, 1995.
(4) Heinrich, R.; Schuster, S. *The regulation of cellular systems*; Chapman & Hall: New York, 1996.
(5) Yetter, R. A.; D F. L.; Rabitz, H. *Combust. Flame* **1985**, *59*, 107.
(6) Cho, S. Y.; Carmichael, G. R.; Rabitz, H. *Atmos. Environ.* **1987**, *21*, 2589.
(7) Susnow, R.; Nachbar, R. B.; Schutt, C.; Rabitz, H. *J. Phys. Chem.* **1991**, *95*, 8585.
(8) Wong, C. F.; Thacher, T.; Rabitz, H. *Rev. Comput. Chem*. **1998**, *12*, 281.
(9) Bleil, R. E.; Wong, C. F.; Rabitz, H. *J. Phys. Chem.* **1995**, *99*, 3379.
(10) Kholodenko, B. N.; Kiyatkin, A.; Bruggeman, F. J.; Sontag, E.; Hoek, J. B. *Proc. Natl. Acad. Sci. U.S.A.* **2002**, *99*, 12841.
(11) Papin, J. A.; Palsson, B. O. *J. Theor. Biol*. **2004**, *227*, 283.
(12) Ingalls, B. P.; Sauro, H. M. *J. Theor. Biol.* **2003**, *222*, 23.
(13) Vojtek, A.; Der, C. J. *J. Biol. Chem.* **1998**, *273*, 19925.
(14) Malumbres, M.; Barbacid, M. *Nature Rev. Cancer* **2003**, *3*, 459.
(15) Hanahan, D.; Weinberg, R. A. *Cell* **2000**, *100*, 57.
(16) Chang, F.; Steelman, L. S.; Lee, J. T.; Shelton, J. G.; Navolanic, P. M.; Blalock, W. L.; Franklin, R. A.; McCubrey, J. A. *Leukemia* **2003**, *17*, 1263.
(17) Huang, C.-Y. F; Farrell, J. E., Jr. *Proc. Natl. Acad. Sci. U.S.A.* **1996**, *93*, 10078.
(18) Bhalla, U. S.; Iyengar, R. *Science* **1999**, *283*, 381.
(19) Kholodenko, B. N.; Demin, O. V.; Moehren, G.; Hoek, J. B. *J. Biol. Chem.* **1999**, *274*, 30169.
(20) Schoeberl, B.; Eichler-Johnsson, C.; Gilles, E. D.; Mueller, G. *Nature Biotechnol.* **2002**, *20*, 370.
(21) Bhalla, U. S.; Ram, P. T.; Iyengar, R. *Science* **2002**, *297*, 1018.
(22) Warne, P.; Viciana, P.; Downward, J. *Nature* **1993**, *36*, 352−355.
(23) Vojtek, A.; Hollenberg, S.; Cooper, J. *Cell* **1993**, *74*, 205.
(24) Aelst, L. V.; Barr, M.; Marcus, M.; Polverino, A.; Wigler, M. *Proc. Natl. Acad. Sci. U.S.A.* **1993**, *90*, 6213.
(25) Egan, S.; Weinberg, R. *Nature* **1993**, *365*, 781.
(26) Lee, J. T., Jr.; McCubrey, J. A. *Leukemia* **2002**, *16*, 486.
(27) Steelman, L. S.; Pohnert, S. C.; Shelton, J. G.; Franklin, R. A.; Bertrand, F. E.; McCubrey, J. A. *Leukemia* **2004**, *18*, 189−218.
(28) Hatakeyama, M.; Kimura, S.; Naka, T.; Kawasaki, T.; Yumoto, N.; Ichikawa, M.; Kim, J.-H.; Saito, K.; Saeki, Shirouzu, M.; M.; Yokoyama, S.; Konagaya, A. *Biochem. J.* **2003**, *373*, 451.
(29) Olayioye, M. A.; Graus-Porta, D.; Beerli, R. R.; Rohrer, J.; Gay, B.; Hynes, N. E. *Mol. Cell. Biol.* **1998**, *18*, 5042.
(30) Sweeney, C.; Lai, C.; Riese, D. J., II; Diamonti, A. J.; Cantley, L. C.; Carraway, K. L., III. *J. Biol. Chem.* **2000**, *275*, 19803.
(31) Reusch, H. P.; Zimmermann, S.; Schaefer, M.; Paul, M.; Moelling, K. *J. Biol. Chem.* **2001**, *276*, 33630.
(32) Dhillon, A. S.; Meikle, S.; Yazici, Z.; Eulitz, M.; Koch, W. *EMBO J.* **2002**, *21*, 64.
(33) Zimmerman, S.; Moelling, K. *Science* **1999**, *286*, 1741−1744.
(34) Moelling, K.; Schad, K.; Bosse, M.; Zimmerman, S.; Schweneker, M. *J. Biol. Chem.* **2002**, *277*, 31099.
(35) Hartwell, L. H.; Hopfield, J. J.; Leibler, S.; Murrray, A. W. *Nature* **1999**, *402*, C47.
(36) Reuven, Y.; Smooke, M. D.; Rabitz, H. *J. Comput. Phys.* **1986**, *64*, 27.
(37) Small, J. R.; Fell, D. A. *J. Theor. Biol.* **1989**, *136*, 181.
(38) Kholodenko, B. N.; Westerhoff, H. V. *FEBS Lett.* **1997**, *414*, 430.
(39) Reder, C. *J. Theor. Biol.* **1998**, *135*, 175.
(40) Press, W. H.; Teukolsky, S. A.; Vetterling, W. T.; Flannery, B. P. *Numerical Recipes in C, The Art of Scientific Computing*, 2nd ed.; Cambridge University Press: Cambridge, U.K., 1992.
(41) Pant, D.; Ghosh, A. *Biophys. Chem.* **2005**, *113*, 275.
(42) Downward, J. *Nature Rev. Cancer* **2003**, *3*, 11.
(43) Sebolt-Leopold, J. S.; Herrera, R. *Nature Rev. Cancer* **2004**, *4*, 937.
(44) Vivanco, I.; Sawyers, C. L. *Nature Rev.* **2002**, *2*, 489.
(45) Workman, P. *Biochem. Soc. Trans.* **2004**, *32*, 393.
(46) Carlson J. M.; Doyle, J. *Proc. Nalt. Acad. Sci. U.S.A.* **2002**, *99*, 2538.
(47) Carlson J. M.; Doyle, J. *Phys. Rev. Lett.* **2000**, *84*, 2529.
(48) Goldbeter, A.; Koshland, D. E., Jr. *Proc. Natl. Acad. Sci. U.S.A.* **1981**, *78*, 6840.
(49) Mayawala, K.; Gelmi, C. A.; Edwards, J. S. *Biophys. J.* **2004**, *87*, L01.
(50) Mutalik, V. K.; Singh, A. P.; Edwards, J. S.; Venkatesh, K. V. *FEBS* **2004**, *558*, 79.